Biological Evaluation of Molecules of the azaBINOL Class as Antiviral Agents: Specific Inhibition of HIV-1 RNase H Activity by 7-Isopropoxy-8-(naphth-1-yl)quinoline

Ross D. Overacker,[1] Somdev Banerjee,[1] George F. Neuhaus,[1] Selena Milicevic Sephton,[1] Alexander Herrmann,[2] James A. Strother,[3] Ruth Brack-Werner,[2] Paul R. Blakemore,[1] and Sandra Loesgen[1]*

[1]Department of Chemistry, Oregon State University, Corvallis, OR 97331, USA.

[2]Institute of Virology, Helmholtz Zentrum München, German Research Center for Environmental Health, Ingolstädter Landstraße 1, D-85764 Neuherberg, Germany

[3]Department of Integrative Biology, Oregon State University, Corvallis, OR 97331, USA.

E-mail: sandra.loesgen@oregonstate.edu

KEYWORDS: azaBINOL, HIV-1 inhibition, HIV reverse transcriptase, RNase H

Abstract

Inspired by bioactive biaryl-containing natural products found in plants and the marine environment, a series of synthetic compounds belonging to the azaBINOL chiral ligand family was evaluated for antiviral activity against HIV-1. Testing of 39 unique azaBINOLs in a single-round infectivity assay resulted in the identification of three promising antiviral compounds, including 7-isopropoxy-8-(naphth-1-yl)quinoline (azaBINOL **B#24**), which exhibited low-micromolar activity. The active compounds and several close structural analogues were further tested against three different HIV-1 envelope pseudotyped viruses as well as in a full-virus replication system (EASY-HIT). Mode-of-action studies using a time-of-addition assay indicated that azaBINOL **B#24** acts after viral entry but before viral assembly and budding. HIV-1 reverse transcriptase (RT) assays that individually test for polymerase and RNase H activity were used to demonstrate that **B#24** inhibits RNase H activity, most likely allosterically. Further binding analysis using bio-layer interferometry (BLI) showed that **B#24** interacts with HIV-1 RT in a highly specific manner. These results indicate that azaBINOL **B#24** is a potentially viable, novel lead for the development of new HIV-1 RNase H inhibitors. Furthermore, this study demonstrates that the survey of libraries of synthetic compounds, designed purely with the goal of facilitating chemical synthesis in mind, may yield unexpected and selective drug leads for the development of new antiviral agents.

1. Introduction

HIV/AIDS continues to be a major global health epidemic. In 2017, there were 36.9 million people living with HIV worldwide and an additional 1.8 million people became newly infected.[1] Despite substantial efforts towards vaccine development, there are currently no FDA-approved vaccines and management of HIV infection requires long-term treatment with potent anti-HIV drugs.[2] Although drug regimens such as antiretroviral therapy (ART) are able to keep HIV viral load low in infected patients, these treatments are typically limited by adverse side effects, increasing drug resistance, high costs, and global availability shortages.[3] Currently, therapeutic antiviral drugs target different phases of the HIV lifecycle including viral attachment, fusion, reverse transcription, integration, and protease activity. Treatments often utilize multiple drugs in combination to combat the rapid emergence of chemoresistant viruses.[3] Therefore, novel therapeutics that act on previously untargeted steps of the viral life cycle are urgently needed to circumvent the onset of drug resistance and to improve treatments.[4]

HIV reverse transcriptase (RT) has been successfully targeted with first and second-generation non-nucleosides reverse transcriptase inhibitors (NNRTIs) as exemplified by nevirapine, first introduced in 1996, and more recently rilpivirine, in 2011.[5, 6] Out of the 27 currently FDA approved HIV drugs on the market, 13 of them target RT polymerase activity, including the NNRTIs.[7] However, the reverse transcriptase enzyme is a multifunctional protein and no drugs have been developed yet that target the RT ribonuclease H (RNase H) activity, which has recently been validated as a target for small molecule drug intervention.[8, 9] HIV RT is responsible for converting the single-stranded viral RNA genome to a double-stranded DNA for subsequent integration into the genome of the host cell. The heterodimeric RT protein (p66/p51) has separate active sites for polymerase and RNase H activity. The polymerase starts the

synthesis of DNA by first copying the viral RNA genome and forming RNA:DNA hybrids while RNase H catalyzes the degradation of RNA in DNA:RNA hybrids to finally form duplex DNA.[10] The RNase H active site contains two bivalent Mg^{2+} ions that chelate and cleave the RNA phosphate backbone by directing a nucleophilic water molecule towards the phosphate linkage.[11] It has been shown that RNase H activity can be abolished through Mg^{2+} chelation in the active site or through allosteric binding near the NNRTI site causing conformational changes.[9] The addition of novel antiviral drugs that target RNase H activity to current combinatorial regimens would introduce a new synergistic method of HIV-1 inhibition greatly improving efficacy of treatment options.

To identify novel leads for drug discovery efforts one may look to sources of compounds that have been either infrequent explored or else untapped in prior studies. Notable in this regard are the numerous ostensibly artificial organic molecules that have been introduced as chiral metal ligands and/or organocatalysts for the purpose of facilitating catalytic enantioselective syntheses. The structural features present in such molecules that are necessary for their intended function (e.g., chiral scaffolds with few rotatable bonds, donor sites from atoms with lone pairs, hydrogen-bond acceptors and donors, sites of localized charge density, zones of steric encumbrance, etc.) could also lead to meaningful and potentially specific interactions with proteins and other classes of biomolecules involved in various diseases. Axially chiral biaryl compounds based on 1,1´-binaphthyl scaffolds are considered a 'privileged' class of reagents for enantioselective synthesis and the principal member of this group, 1,1´-bi-2-naphthol (BINOL, **1**), has become one of the most widely used ligands for stoichiometric and catalytic asymmetric reactions.[12] While BINOL itself has previously been found to be cytotoxic, many other biaryl compounds, either found in nature or of artificial origin, have shown potent and selective bioactivities.[13,14] For example, the

84 axially chiral dimeric naphthylisoquinolone alkaloids first isolated from *Anicistrocladus*
85 *korupensis* in 1991 and later named the michellamines, exhibit selective anti-HIV activity.[15-19]
86 Given these facts taken together with the existence of other antiviral biaryl natural products (e.g.,
87 dioncophylline[20]) and recently identified synthetic antiviral drug leads with multiple aromatic
88 ring systems (e.g., arbidol,[21] peptide triazoles,[22] rhodanine derivatives,[23] naphthylhydrazones,[24]
89 and hydroxypyridones[25]), we elected to test a library of heterocyclic biaryl compounds available
90 to us and belonging to the so-called 'azaBINOL' chiral ligand family for inhibition of HIV-1
91 infection.

92 The azaBINOLs are nitrogenous analogs of BINOL based on isostructural 8-(naphth-1-
93 yl)quinoline (**2**, 8-azaBINOL)[26] and 8,8'-biquinolyl (**3**, 8,8´-diazaBINOL)[27-29] motifs (Figure 1).
94 These molecules have been a focus of interest both from a fundamental standpoint[26, 30, 31] and for
95 their potential utility in enantioselective synthesis,[32, 33] but prior to this work, studies of any
96 aspect of the biological activity of azaBINOLs had yet to be reported. Herein, we show that
97 deoxy-8-azaBINOL derivatives provide a novel scaffold for the inhibition of HIV-1 RT RNase H
98 activity. Our lead compound, the isopropyl ether derivative of 2'-deoxy-8-azaBINOL (**B#24**),
99 shows unoptimized low micromolar activity (4-9 μM range) in an HIV single round infectivity
100 assay as well as in fully infectious viral assays with low cytotoxicity and a selectivity index
101 of 14.

102

2. Chemistry

A significant advantage of the azaBINOL family of molecules as compared to their all carbocyclic BINOL congeners is the ease of derivatization of the quinoline nucleus and therefore the facility with which essentially any position of azaBINOL scaffolds can be decorated with ancilliary functionality.[29] Of the six compounds of primary interest herein (*vide infra*, see Figure 2), only the quinol-type 2′-deoxy-8-azaBINOL carbamate derivative **B#43** was previously described in the literature.[26] The five new compounds were prepared from known deoxy azaBINOLs (**4**, **5**, and **6**) via straightforward alkylation and acylation reactions (Scheme 1). Carbamate **B#43**, itself accessed by Suzuki-Miyauri cross-coupling of an 8-iodoquinoline and 1-naphthaleneboronic acid,[26] was converted to isopropyl ether **B#24** by saponification to quinol **4** followed by Williamson ether synthesis (Scheme 1). The other four compounds, naphthol-type 2-deoxy-8-azaBINOL derivatives **B#59** and **B#60** and 2-deoxy-8,8′-diazaBINOL derivatives **B#57** and **B#58**, were prepared from the corresponding phenols **5** and **6**. As hitherto reported, phenols **5** and **6** are themselves efficiently prepared by N-directed oxidative CH functionalization of 8-(naphth-1-yl)quinoline[26] and 8,8′-biquinolyl,[29] respectively. All six of the azaBINOLs of main focus were prepared and tested for biological activity in racemic form. The configurational stability of these axially chiral compounds has yet to be determined, however, their racemization half-lives are likely to be significantly higher than those of quinol **4** [$\tau_{1/2(rac.)}$ = 120 h in MeOH at 24 °C] and naphthol **5** [$\tau_{1/2(rac.)}$ = 89 h in MeOH at 24 °C] which have been measured as indicated.[26]

3. Results

3.1 HIV-1 *in vitro* activity screening of azaBINOL compounds

A library of 39 unique azaBINOLs and two BINOLs was screened for antiviral HIV-1 activity using a pseudo-typed viral particle, single round infectivity assay (HIVpp) (see Supporting Information for full screening data and structures of all library members; all compounds were screened in racemic form and four were additionally evaluated as their enantiopure (*aS*)- and (*aR*)-atropisomers). Antiviral activity was compared directly to compound cytotoxicity using a standard MTT-based cell viability assay to assess selectivity indices of compounds. Initial screening efforts at single-dose concentrations (10 μg/mL) of the full compound library revealed three compounds with low micromolar anti-HIV activity: **B#24**, **B#43**, and **B#60** (Figure 2). These compounds, an isopropyl ether (**B#24**) and two carbamate derivatives (**B#43** and **B#60**) of deoxy-8-azaBINOL molecules, showed high viral inhibitory activity with only minor cytotoxicity and warranted further investigation. Closer analysis of the compound library revealed three additional azaBINOLs sharing similar structural features to the aforementioned active compounds: a naphthol-type regioisomer of quinol-type ether **B#24** (**B#59**), as well as 2-deoxy-8,8′-diazaBINOL congeners of the isopropyl ethers and carbamates (**B#57** and **B#58**). Despite the close structural similarities of these compounds, they showed little antiviral activity as compared to **B#24**, **B#43**, and **B#60** (Figure 2). HIV antiviral activity was evident for the isopropyl ether and carbamate derivatives of 2- and 2′-deoxy-8-azaBINOL but it was notably completely absent for the corresponding 2-deoxy-8,8′-diazaBINOL series of compounds. Due to the close structural similarities between the active isopropyl ether and carbamate compounds to their non-active counterparts in the HIVpp assay, we decided to move all six compounds forward for further activity explorations.

Antiviral activity of the isopropyl ether compounds **B#24, B#59, B#57** and the carbamate derivatives **B#43, B#60,** and **B#58** was assessed against three different HIV-1 enveloped pseudo-

typed particles with differing tropism including HXB2, YU2, and 89.6 (Table 1). All six of the azaBINOL compounds showed similar activities across all viral variants. Quinol-type 2′-deoxy-8-azaBINOL ether **B#24** in particular showed low micromolar HIV-1 neutralization against each of the strains tested with activity similar to other antiviral drugs such as abacavir.[34] Although the naphthol-type 2-deoxy-8-azaBINOL ether **B#59** did show minor antiviral activity at high concentrations, its IC_{50} was greater than the concentrations tested and significantly larger in comparison to the closely related quinol-type ether **B#24**, which has an IC50 value of 4 - 8 μM. The significant difference in antiviral activity of these two regioisomers (**B#24** and **B#59**) hints towards a highly specific and selective mode of inhibition. The corresponding carbamate derivatives of deoxy-8-azaBINOLs, **B#43** and **B#60**, both showed moderate antiviral activity against all three viral strains but with smaller selectivity indices. Again, neither of the 2-deoxy-8,8′-diazaBINOL derivatives, **B#57** or **B#58**, showed any antiviral activity at concentrations up to 200 μM.

Next we used the EASY-HIT full viral infection assay system[35] to test all six isopropyl ether and carbamate azaBINOL derivatives against fully-infectious, replication competent HIV-1_{LAI} (Table 2). The quinol-type 2′-deoxy-8-azaBINOL ether **B#24** continued to exhibit low micromolar antiviral activity in the EASY-HIT assay system in accordance with results obtained from the HIVpp assay. Surprisingly, the naphthol-type 2-deoxy-8-azaBINOL ether **B#59** exhibited increased antiviral activity. The deoxy-8-azaBINOL carbamate derivatives **B#43** and **B#60** gave similar high micromolar viral neutralization but also displayed comparable cytotoxicity. The analogous 2-deoxy-8,8′-diazaBINOL compounds, **B#57** and **B#58**, showed no antiviral activity or cytotoxicity at concentrations tested up to 200 μM.

Out of the 41 unique compounds originally screened for anti-HIV-1 activity, one compound, quinol-type 2′-deoxy-8-azaBINOL ether **B#24**, stands out with selective antiviral activity and a favorable selectivity index. Small changes to its structure, including moving the isopropyl ether substituent to the naphthyl ring system (**B#59**), or the introduction of an additional aromatic ring-bound nitrogen atom (**B#57**), results in drastically reduced antiviral activity. While the deoxy-8-azaBINOL carbamate derivatives **B#43** and **B#60** do exhibit antiviral activity in the phenotypic assays, they also show significant cytotoxicity and therefore their apparent antiviral activity is likely due to interference with the cell-based assay. The low micromolar antiviral activity of lead compound **B#24** encouraged us to explore its mode-of-action.

3.2 AzaBINOLS are not pan-assay interference compounds (PAINS)

Promiscuous inhibitors in high-throughput screening endeavors often lead to unproductive identification and development of compounds with non-specific activity.[36] For example, cell-based assays requiring a colorimetric out-read can be inhibited through non-specific mechanisms giving false-positive results.[37] The cell-based HIVpp used in this study contains a luciferase reporter out read, so we looked to test the capacity of **B#24** to directly inhibit luciferase luminescence in a recombinant luciferase enzyme test (SI Figure 6).[38] **B#24** showed no inhibition of luciferase activity nor quenching at any concentrations tested verifying that it was not acting on luminescence. Additionally, based on the low solubility and largely hydrophobic surface area of **B#24**, we sought to probe its ability to inhibit HIV-1 through unspecific aggregation effects. We tested the ability for **B#24** to aggregate at higher concentrations in aqueous conditions via an ^{1}H-NMR dilution study (SI Figure 7).[39] Five concentrations of **B#24** were tested from 200 µM to 12 µM in 50 mM phosphate buffer made with D_2O and 1% DMSO-d6. No changes were seen in

the number of resonances, peak shape, or chemical shift values indicating that **B#24** does not aggregate under the test conditions.

3.3 Time-of-addition assay

The single round infectivity assay using HIV-1 enveloped pseudotyped viruses is able to report on inhibition of early stages of infection including cell entry, reverse transcription, and integration steps. The active azaBINOL compound **B#24** inhibited all HIV-1 strains tested regardless of their differing viral tropism (HXB2, YU2, and 89.6). This broad inhibition indicated that the antiviral mode-of-action is unlikely to rely on the viral fusion process, as changing the surface glycoprotein does not affect antiviral activity. Additionally, the EASY-HIT assay indicated that **B#24** is active prior to viral packing and budding. To further delineate the stage of the virus replication cycle inhibited by **B#24**, a time-of-addition assay was performed using HIV-1 pseudotyped particles. Compound **B#24** as well as the standard inhibitors temsavir and efavirenz were added at different time points post exposure of the cell to virus to evaluate their inhibitory activity throughout viral infection (Figure 3). Our results show that **B#24** does not act on the initial viral-entry step when compared to the activity of HIV-1 entry inhibitor temsavir, which loses activity if dosed post viral entry. Instead, **B#24** remains active throughout the assay, but exhibits a subtle decrease in antiviral activity between 6-8 hours post infection. Next, we sought to explore viral enzyme interactions directly to verify if **B#24** interacts with the HIV RT dual functions (DNA polymerase and/or RNase H activity) or HIV integrase.

3.4 Activity of B#24 against HIV-1 reverse transcriptase

NNRTI binding to the HIV RT enzyme occurs at a distant, allosteric binding site and the long-distance effects on the RT polymerase activity are well documented.[10] In contrast, inhibitors of the HIV RT enzyme that target its RNase H function directly affect the catalytic side with its

Mg^{2+} ions, and therefore are often dual inhibitors, with effects on reverse transcriptase and integrase as both require bivalent metals in their active site. We screened **B#24** for inhibitory activity in recombinant protein-based assays to test for HIV-1 RT and/or integrase antiviral inhibition (Table 3). AzaBINOL **B#24** showed no effect against HIV-1 integrase activity in a commercially available kit (ExpressBio, Frederick, MD) at any concentration tested up to 200 μM. When tested against an HIV-1 RT polymerase assay we observed only weak inhibitory effects for **B#24** at concentrations higher than 100 μM, several orders of magnitude weaker than seen in our cell-based assays.

However, since RNase H activity, the second catalytic activity of the HIV-1 reverse transcriptase, is not detected in the above RT-polymerase assay, we investigated the effect of **B#24** on RNase H activity using a previously reported FRET based approach.[40, 41] Here, we used a pair of oligonucleosides including an 18-mer strand of RNA containing a 3'-fluorescein modification and an 18-mer strand of DNA with a 5'-dabcyl quencher modification. When RNA is cleaved from the RNA/DNA hybrid by RNase H activity, the fluorescent probe is removed from its quenching partner (dabcyl) resulting in fluorescence. We found that **B#24** inhibited RNase H activity of HIV RT with an IC_{50} of 14.2 μM, within the same range as the low micromolar cell-based assay results (Table 3).

Several classes of compounds have shown promising antiviral activity by acting on RNase H activity including N-hydroxyimides,[42] tropolones,[43, 44] hydroxypyridonecarboxylic acids,[25, 45, 46] diketoacids,[47] vinylogous ureas,[48] and thienopyrimidinones;[49] the majority of which target the active site of RNase H through Mg^{2+} ion chelation. With this in mind, we sought to probe whether azaBINOL **B#24** was inhibiting RNase H via the active site using a Mg^{2+} ion chelation and absorbance test. Mg^{2+} ions present in the active site of RNase H are an integral part of its

endonuclease function and various inhibitors have been shown to interfere with their chelating properties.[8, 9] Compound **B#24** was tested for Mg^{2+} binding by assessment of its UV absorption under an increasing concentration of Mg^{2+} following existing procedures.[50] No UV absorbance changes were observed with the addition of Mg^{2+} up to 120 mM with **B#24** (100 μM) (Figure 4). Therefore, we conclude that **B#24** is not interacting with Mg^{2+} ions and subsequently is not directly inhibiting RNase H activity through active site binding. Instead, it is likely that **B#24** inhibits RNase H enzyme activity allosterically, without affecting the polymerase function of RT. The azaBINOL compound **B#24** adds a new structural class to emerging group of selective HIV RNase H inhibitors including dihydroxy benzoyl naphthyl hydrazone (DHBNH),[24] various derivatives of vinylogous ureas,[48, 51] as well as cycloheptathiophene-3-carboxamides (cHTC).[52, 53] Allosteric binding may exhibit fewer side effects compared to active site Mg^{2+} chelating inhibitors and therefore allow for a more favorable therapeutic window.[8, 9]

3.5 HIV-1 reverse transcriptase binding

To show that **B#24** inhibits RNase H activity by binding the HIV-1 reverse transcriptase enzyme, we explored direct binding to immobilized HIV-1 RT using bio-layer interferometry (BLI). BLI allows for the real time measurement of binding affinities between ligands and analytes of varying size using single-use, fiber optical sensors. BLI measures association (k_{on}) and dissociation (k_{off}) rates directly from full spectrum wavelength shifts associated with interference pattern changes derived from binding events at a sensors tip to determine binding affinities (K_D).[54] Recombinant-wild type HIV-1 p66/p51 RT (NIH Aids Reagents) was immobilized via amine coupling onto BLI biosensors. **B#24**, selected other azaBINOLs, and control compounds (rilpivirine positive control, raltegravir negative control) were prepared in 1x kinetics buffer at multiple concentrations. Each compound was tested at multiple concentrations,

responses were globally fit using a 1:1 binding model, and these fits were used to calculate K_D values. The binding curves obtained for **B#24** are shown in Figure 5. In good agreement with cell-based antiviral assays, **B#24** shows a concentration-dependent binding to HIV-1 RT. Control compound rilpivirine also showed concentration dependent binding curves while raltegravir, an HIV-1 integrase inhibitor showed no binding at any concentration tested as expected (SI Figure 4). Although the acquired K_D of 38 μM associated with **B#24** is higher than the IC_{50} in cell-based assays, it should be noted that the affinity value cannot be directly related to neutralization efficacy, as seen in many high-affinity, non-neutralizing HIV antibodies.[55-57] No binding was observed for the related azaBINOLs of interest from the compound library (SI Figure 7). In summary, the BLI binding data obtained reveals a striking correlation between the binding affinity of **B#24** towards its target HIV RT and its antiviral activity.

4. Discussion and conclusion

RNase H inhibition of HIV-1 RT is an under explored and under-utilized mechanism of inhibition. The azaBINOL compounds reported here represent novel scaffolds that inhibit HIV via an underexplored allosteric mechanism with low toxicity and high specificity. In particular, the isopropyl ether derivative of 2′-deoxy-8-azaBINOL (**B#24**) exhibits with potent and specific antiviral activity against HIV RNase H. We utilized time-of-addition experiments and recombinant enzyme assays to show that **B#24** specifically inhibits RNase H. In addition, we used BLI to show that **B#24** binds to HIV RT via a 1:1 binding mechanism with a binding affinity (K_D) of 38 μM. Although a number of azaBINOL compounds within the screened library were found to have limited solubility in the cell-based assays as expected, aggregation and non-specific inhibition was tested thoroughly and can be dismissed for lead compound **B#24** (SI Fig 6,7).

Clinically approved HIV-1 NNRTI's including nevirapine, efavirenz, and recently rilpivirine, exhibit antiviral activity against HIV-1 by allosterically inhibiting RT through hydrophobic interactions at the NNRTI binding site.[24, 25, 58, 59] Binding to the NNRTI binding site often results in combined effects in inhibiting DNA polymerase and RNase H activity through conformational shifts in the enzyme.[60] Only a few privileged structures like the acyl hydrazones,[24] vinylogous ureas,[48] cHTC's,[53] and now **B#24** have been identified with potent HIV-1 inhibitory effects through specific RNase H inhibition.

We predict that the naphthyl moiety of the azaBINOL compounds may bind to a hydrophobic surface present on the RNase H domain of HIV-1 RT[25] while leaving the substituted quinoline space to further interact with the protein. In the case of the 2-deoxy-8,8′-diazaBINOL derivatives (**B#57**, **B#58**) or the naphthol-type regioisomer of ether **B#24** (**B#59**), the antiviral activity is absent or significantly reduced likely due to the reduced hydrophobic surface and increased steric interactions, respectively. Ongoing research in our laboratory will explore if **B#24** truly binds allosterically to RNase H and if the binding affinity and HIV-1 neutralization can be enhanced by chemical modifications.

Future studies are planned to optimize the azaBINOL core structure to increase HIV-1 activity by improving HIV-1 binding, solubility, and to reduce cytotoxicity. It is anticipated that the absolute configuration of the biaryl system will influence biological activity but to what extent remains an open question since a majority of the compounds evaluated herein were tested in racemic form only. Work is in progress to determine the configurational stability of compounds such as **B#24** and bioassays of these materials in enantioenriched form will be conducted should their racemization half-lives prove to be high enough for such an effort to be meaningful.

In summary, we discovered that an isopropyl ether derivative of an aza-analog of the archetypal axially chiral biaryl ligand BINOL, inhibits HIV-1 infection in vitro. Based on the identified RNase H inhibition, direct HIV-1 RT binding, and the known hydrophobic binding surfaces associated with allosteric inhibiton,[58] we believe that **B#24** is a novel allosteric inhibitor of HIV-1 RT-RNase H activity. While biaryl compounds of natural origin have long been known to exhibit significant biological activity,[14, 61] this study suggests that further investigations of the bioactivity of artificial biaryls, designed purely with synthetic utility in mind, are warranted.

5. Experimental Section

5.1 General experimental procedures.

UV spectra, luminescence and absorbance readings were recorded on a BioTek Synergy HT plate reader. NMR spectra were acquired on Bruker Avance III 400 MHz, Bruker Avance III 500 MHz, Bruker Avance III 700 MHz, and Bruker Ascend 800 MHz spectrometers, equipped with either a 5 mm TXI probe (500 MHz), a 5 mm BBO probe (400 MHz and 500 MHz), or a 5 mm TCI cryoprobe (700 MHz and 800 MHz), with the appropriate solvent signals used as an internal calibration standard [for $CDCl_3$: δ_H ($CHCl_3$) = 7.26 ppm, δ_C ($CDCl_3$)= 77.2 ppm]. Numbers in parentheses following carbon atom chemical shifts refer to the number of attached hydrogen atoms as revealed by the DEPT spectral editing technique. Infra-red spectra were recorded on a Perkin Elmer Spectrum II FT-IR using a thin film between NaCl plates. Low (MS) and high resolution (HRMS) mass spectra were obtained using electrospray (ES) ionization on a Waters SYNAPT instrument interfaced with a Shimadzu LC20ad liquid chromatograph. Ion mass/charge (*m/z*) ratios are reported as values in atomic mass units. Preparative chromatographic separations were performed on silica gel 60 (35-75 μm) and reactions were

329 followed by TLC analysis using silica gel 60 plates (2-25 μm) with fluorescent indicator (254
330 nm) and visualized by UV or phosphomolybdic acid (PMA).

331 **5.2 Materials.**

332 Non-commercially available BINOL and azaBINOL compounds tested were previously
333 synthesized and characterized at Oregon State University. Preparation details and
334 characterization data for previously undescribed compounds (**B#24**, **B#57**, **B#58**, **B#59**, and
335 **B#60**) are given below. Unless otherwise stated, all solvents were purchased from ThermoFisher
336 Scientific (Waltham, MA) and reagents for chemical synthesis were purchased from Sigma-
337 Aldrich (Milwaukee, WI) and used as received. TZM-bl cells and the HIV-1 inhibitors
338 raltegravir, efavirenz, and rilpivirine were obtained through the NIH Aids Reagent Program.[62-67]
339 HEK 293T cells were a kind gift from Dr. Pastey Manoj (Oregon State University). HIV-1 viral
340 expression plasmids (pSG3, pHxB2, and pYU2) were obtained as a generous gift from Carole
341 Bewley (NIH, NIDDK). Dulbeco's modified eagle medium (DMEM) was purchased from VWR.
342 PBS buffer was purchased from Gibco (ThermoFisher Scientific). Trypsin/EDTA (0.25%/2.21
343 mM) and penicillin/streptomycin solutions were attained from Corning Life Sciences (Corning,
344 NY). Fetal Bovine Serum (FBS) was obtained from Atlanta Biologicals (Flowery Branch, GA).
345 QuantiLum Recombinant Luciferase and the BrightGlo Luciferase Assay System were acquired
346 from Promega (Madison, WI). The HIV-1 inhibitor temsavir was acquired from ViiV Healthcare
347 (Brentford, UK). All compounds received were tested for purity and identity via LCMS analysis
348 before use.

349 **5.3 Synthesis of new compounds and characterization data.**

350 *Representative procedure for preparation of isopropyl ethers.* **7-(Isopropyloxy)-8-(naphth-**
351 **1-yl)quinoline (B#24)**: A stirred solution of 7-hydroxy-8-(naphth-1-yl)quinoline (**4**, 20 mg,

0.074 mmol)[26] in reagent grade DMF (0.5 mL) at rt under Ar was treated with NaH (12 mg, 60 wt.% in mineral oil, 0.30 mmol). Effervescence was observed. After stirring for 30 min, neat 2-bromopropane (0.030 mL, d = 1.31, 39 mg, 0.317 mmol) was added. The reaction mixture was then heated to 45 °C and stirring continued for 18 h. After this time, the mixture was allowed to cool to rt and partitioned between EtOAc (5 mL) and H_2O (5 mL). The aqueous phase was extracted with EtOAc (5 mL) and the combined organic phases were washed with H_2O (5 mL) and brine (5 mL), then dried (Na_2SO_4) and concentrated *in vacuo*. The residue was purified by column chromatography (SiO_2, eluting with 15-30% EtOAc in hexanes) to afford ether **B#24** (20 mg, 0.064 mmol, 86%) as a colorless oil: IR (neat) 2976, 2927, 1610, 1498, 1307, 1259, 1111, 773 cm^{-1}; ^1H NMR (400 MHz, $CDCl_3$) δ 8.76 (1H, dd, J = 4.2, 1.8 Hz), 8.17 (1H, dd, J = 8.2, 1.8 Hz), 7.92 (1H, dm, J = 8.3 Hz), 7.90 (2H, d, J = 9.0 Hz), 7.61 (1H, dd, J = 8.2, 7.0 Hz), 7.47 (1H, d, J = 9.0 Hz), 7.45 (1H, dd, J = 7.0, 1.2 Hz), 7.42 (1H, ddd, J = 8.1, 6.7, 1.4 Hz), 7.31-7.21 (3H, m), 4.42 (1H, septet, J = 6.1 Hz), 1.05 (3H, d, J = 6.1 Hz), 0.98 (3H, d, J = 6.1 Hz) ppm; ^{13}C NMR (175 MHz, $CDCl_3$) δ 157.6 (0), 150.2 (1), 147.0 (0), 137.9 (0), 133.9 (0), 132.9 (0), 129.1 (1), 128.9 (1), 128.5 (1), 128.3 (1), 126.2 (1), 125.8 (1), 125.6 (1), 125.5 (1), 124.1 (0), 119.0 (1), 118.5 (1), 72.6 (1), 22.3 (3), 22.2 (3) ppm (aromatic C-atom signals not fully resolved, 20 peaks observed for 22 unique C-atoms); MS (ES+) *m/z* 314 $(M+H)^+$; HRMS (ES+) *m/z* 314.1544 (calcd. for $C_{22}H_{20}NO$: 314.1545).

7-(Isopropyloxy)-8,8′-biquinolyl (B#57): 7-Hydroxy-8,8′-biquinolyl (**6**, 52 mg, 0.191 mmol)[29] was converted into isopropyl ether **B#57** (46 mg, 0.146 mmol, 77%) by analogy to the synthesis of **B#24** given above. Data for **B#57**: colorless oil; IR (neat) 2925, 1658, 1596, 1496, 1272, 1112, 1045, 829, 796 cm^{-1}; ^1H NMR (400 MHz, $CDCl_3$) δ 8.78 (1H, dd, J = 3.9, 1.8 Hz), 8.72 (1H, dd, J = 4.2, 1.8 Hz), 8.21 (1H, dd, J = 8.3, 1.8 Hz), 8.14 (1H, dd, J = 8.2, 1.8 Hz), 7.90

(1H, dd, 7.2, 2.5 Hz), 7.88 (1H, d, J = 9.1 Hz), 7.71-7.65 (2H, m), 7.47 (1H, d, J = 9.0 Hz), 7.34 (1H, dd, J = 8.3, 4.2 Hz), 7.22 (1H, dd, J = 8.2, 4.2 Hz), 4.46 (1H, septet, J = 6.1 Hz), 1.06 (3H, d, J = 6.1 Hz), 0.96 (3H, d, J = 6.1 Hz) ppm; ^{13}C NMR (100 MHz, $CDCl_3$) δ 156.6 (0), 150.7 (1), 149.9 (1), 148.8 (0), 147.8 (0), 136.4 (0), 136.3 (1), 136.0 (1), 132.2 (1), 128.8 (1), 128.6 (0), 127.7 (1), 127.3 (0), 126.3 (1), 124.2 (0), 120.7 (1), 119.0 (1), 118.2 (1), 72.5 (1), 22.5 (3), 22.3 (3) ppm; MS (ES+) *m/z* 315 $(M+H)^+$; HRMS (ES+) *m/z* 315.1502 (calcd. for $C_{21}H_{19}N_2O$: 315.1497).

2-(Isopropyloxy)-1-(quinol-8-yl)naphthalene (B#59): 2-Hydroxy-1-(quinol-8-yl)naphthalene (**5**, 75 mg, 0.276 mmol)[26] was converted into isopropyl ether **B#59** (66 mg, 0.211 mmol, 76%) by analogy to the synthesis of **B#24** given above. Data for **B#59**: colorless oil; IR (neat) 2976, 2927, 1716, 1593, 1496, 1371, 1235, 798, 750 cm^{-1}; ^{1}H NMR (400 MHz, $CDCl_3$) δ 8.80 (1H, dd, J = 4.2, 1.8 Hz), 8.24 (1H, dd, J = 8.3, 1.8 Hz), 7.94-7.88 (2H, m), 7.84 (1H, dm, J = 8.1 Hz), 7.68-7.64 (2H, m), 7.41 (1H, d, J = 9.0 Hz), 7.37 (1H, dd, J = 8.3, 4.2 Hz), 7.31 (1H, ddd, J = 8.0, 6.6, 1.4 Hz), 7.21 (1H, ddd, J = 8.5, 6.6, 1.3 Hz), 7.15 (1H, dm, J = 8.5 Hz), 4.36 (1H, septet, J = 6.1 Hz), 1.05 (3H, d, J = 6.1 Hz), 0.89 (3H, d, J = 6.1 Hz) ppm; ^{13}C NMR (175 MHz, $CDCl_3$) δ 153.5 (0), 150.3 (1), 147.8 (0), 136.9 (0), 136.3 (1), 134.4 (0), 132.5 (1), 129.6 (0), 129.4 (1), 128.6 (0), 128.1 (1), 127.7 (1), 126.3 (1), 126.1 (1), 126.0 (0), 125.9 (1), 123.7 (1), 121.0 (1), 118.5 (1), 72.9 (1), 22.6 (3), 22.4 (3) ppm; MS (ES+) *m/z* 314 $(M+H)^+$; HRMS (ES+) *m/z* 314.1546 (calcd. for $C_{22}H_{20}NO$: 314.1545).

Representative procedure for preparation of carbamates. **7-[(Diethylamino)carbonyloxy]-8,8´-biquinolyl (B#58)**: A stirred solution of 7-hydroxy-8,8´-biquinolyl (**6**, 43 mg, 0.158 mmol)[29] in pyridine (1.0 mL) at rt under Ar was treated with neat diethylcarbamoyl chloride (0.080 mL, d = 1.07, 86 mg, 0.632 mmol). The resulting solution was heated to 100 °C and

stirred for 24 h. After this time, the mixture was allowed to cool to rt and partitioned between EtOAc (10 mL), H_2O (15 mL) and sat. aq. $NaHCO_3$ (5 mL). The aqueous phase was extracted with EtOAc (10 mL) and the combined organic phases washed with H_2O (5 mL) and brine (5 mL), then dried (Na_2SO_4) and concentrated *in vacuo*. The residue was purified by column chromatography (SiO_2, eluting with 3% MeOH in CH_2Cl_2) to afford carbamate **B#58** (45 mg, 0.121 mmol, 77%) as a colorless oil: IR (neat) 2930, 1715, 1594, 1417, 1263, 1208, 1157, 796 cm^{-1}; ^1H NMR (400 MHz, $CDCl_3$) δ 8.81 (1H, dd, J = 4.3, 1.7 Hz), 8.79 (1H, dd, J = 4.2, 1.7 Hz), 8.22 (1H, dd, J = 6.6, 1.7 Hz), 8.20 (1H, dd, J = 6.5, 1.7 Hz), 7.94 (1H, d, J = 8.9 Hz), 7.90 (1H, dd, J = 8.1, 1.3 Hz), 7.76 (1H, dd, J = 7.1, 1.4 Hz), 7.68 (1H, dm, J = 7.3 Hz), 7.64 (1H, d, J = 8.8 Hz), 7.35 (1H, t, J = 4.4 Hz), 7.33 (1H, d, J = 4.4 Hz), 3.17-3.06 (2H, m), 2.68 (1H, dq, J = 14.2, 7.1 Hz), 2.49 (1H, dq, J = 14.2, 7.0 Hz), 0.95 (3H, t, J = 7.0 Hz), 0.32 (3H, t, J = 7.0 Hz) ppm; ^{13}C NMR (100 MHz, $CDCl_3$) δ 153.8 (0), 150.7 (1), 150.3 (1), 150.1 (0), 148.4 (0), 147.5 (0), 136.2 (1), 136.2 (1), 135.0 (0), 132.4 (1), 130.4 (0), 128.6 (0), 128.4 (1), 128.1 (1), 126.6 (0), 126.3 (1), 123.4 (1), 120.9 (1), 120.4 (1), 41.9 (2), 41.2 (2), 13.3 (3), 13.2 (3) ppm; MS (ES+) *m/z* 372 $(M+H)^+$; HRMS (ES+) *m/z* 372.1716 (calcd. for $C_{23}H_{21}N_3O_2$: 372.1712).

2-[(Diethylamino)oxycarbonyl]-1-(quinol-8-yl)naphthalene (B#60): 2-Hydroxy-1-(quinol-8-yl)naphthalene (**5**, 50 mg, 0.184 mmol)[26] was converted into carbamate **B#60** (59 mg, 0.159 mmol, 86%) by analogy to the synthesis of **B#58** given above. Data for **B#60**: colorless oil; IR (neat) 2973, 2931, 1713, 1419, 1269, 1213, 1159, 982, 799, 750 cm^{-1}; ^1H NMR (400 MHz, $CDCl_3$) δ 8.83 (1H, dd, J = 4.2, 1.8 Hz), 8.23 (1H, dd, J = 8.3, 1.8 Hz), 7.96 (1H, d, J = 8.9 Hz), 7.92 (1H, dd, J = 8.1, 1.5 Hz), 7.91 (1H, dm, J = 8.2 Hz), 7.74 (1H, dd, J = 7.1, 1.5 Hz), 7.65 (1H, dd, J = 8.1, 7.2 Hz), 7.52 (1H, d, J = 8.9 Hz), 7.42 (1H, ddd, J = 8.1, 6.3, 1.6 Hz), 7.39 (1H, dd, J = 8.2, 4.2 Hz), 7.33-7.24 (2H, m), 3.15-3.08 (2H, m), 2.74 (1H, dq, J = 13.9, 6.9 Hz), 2.53

(1H, dq, J = 14.2, 7.3 Hz), 0.94 (3H, t, J = 7.0 Hz), 0.32 (3H, t, J = 6.9 Hz) ppm; ^{13}C NMR (100 MHz, $CDCl_3$) δ 154.2 (0), 150.4 (1), 147.2 (2C, 0), 136.7 (1), 135.4 (0), 134.0 (0), 132.6 (1), 131.8 (0), 129.2 (1), 128.6 (2C, 0), 128.3 (1), 128.1 (1), 126.5 (1), 126.3 (1), 126.2 (1), 125.1 (1), 122.5 (1), 121.2 (1), 42.0 (2), 41.3 (2), 13.3 (2C, 3) ppm; MS (ES+) *m/z* 371 $(M+H)^+$; HRMS (ES+) *m/z* 371.1761 (calcd. for $C_{24}H_{23}N_2O_2$: 371.1760).

5.4 Cell culture.

TZM-bl and HEK 293T cells were grown in DMEM supplemented with 10% (v/v) FBS, penicillin (100 units/mL), and streptomycin (100 μg/mL). Cells were maintained in a humidified incubator at 37°C with 5% CO_2. The passage number of cells used in experiments never exceeded 20 passages. All cell lines were tested mycoplasma-negative by real-time PCR (MycoSolutions mycoplasma detection kit, Akron Biotech, Boca Raton, FL).

5.5 Pseudovirus production.

HIV-1 pseudotyped viruses were prepared as previously described.[68] Briefly, HEK 293T cells were transfected with an envelope expression plasmid (pHxB2, pYU2, or p89.6) and an envelope deficient HIV-1 backbone vector ($pSG3_{\Delta env}$) using XtremeGENE HP DNA Transfection Reagent (Roche). After 24 hours of incubation at 37°C and 5% CO_2, the growth media was replaced with fresh media followed by an additional 24 hours of incubation. Cellular supernatant was collected and passed through a 0.45 μm filter to give pseudoviral stock. 1 mL pseudoviral aliquots were stored at -80°C until further use in neutralization assays. Viral strength was determined through $TCID_{50}$ calculations. TZM-bl cells were plated at 9000 cells per well in white 96 well plates (Greiner Bio-One) and incubated at 37 C, 5% CO_2 for 24 hours. HIV-1 pseudoviruses were added over a two-fold dilution series to wells. At 48 hours-post infection, cells were lysed and BrighGlo luciferase substrate (Promega) added. Luminescence reading were

444 immediately recorded and the $TCID_{50}$ value calculated as 50% of the maximum light output
445 based on control wells.

446 **5.6 HIV-1 pseudovirus single-round infectivity assay**.

447 Viral infection rates of HIV-1 pseudoviruses in the presence of inhibitors was measured
448 through HIV-1 pseudoviral tat-induced luciferase production in TZM-bl cells as described
449 previously.[68] TZM-bl cells were plated at 9000 cells/well into 96 well plates (excluding outer
450 wells to avoid edge effects) followed by overnight incubation at 37°C, 5% CO_2. Inhibitors and
451 pseudoviral particles at a final concentration of 1x (based on $TCID_{50}$ measurements) were
452 incubated together for 20 min prior to transfer to adherent TZM-bl cells followed by 48 hours
453 incubation at 37°C, 5% CO_2. Viral infection was quantified based on luminescent readings taken
454 immediately after the addition of BrighGlo luciferin substrate to infected cells in lysis buffer and
455 relative infectivity rates calculated based on infectious and noninfectious vehicle control wells
456 (1% DMSO). Antiviral IC_{50} values were calculated from compound dilution series ran in
457 triplicate.

458 **5.7 HIV Full virus Screening (EASY-HIT).**

459 The EASY-HIT assay[35] is based on HIV-1 susceptible reporter cells (LC5-RIC) that contain
460 a stably integrated fluorescent reporter gene that is activated upon successful HIV-1 infection
461 and expression of the early viral protein Rev and Tat. Briefly, LC5-RIC cells were seeded into
462 black 96-well plates at a density of 10,000 cells per well 24 hours prior to infection. Compounds
463 stocks dissolved at 20 mM in DMSO were screened at multiple concentrations from 0.1 to 200
464 µM at a final DMSO concentration of 1% to establish IC_{50} curves. After compound addition,
465 LC5-RIC cells were infected by adding HIV-1 inoculum at an MOI of 0.5 to each well of the
466 plate. Cells were incubated at 37°C, 5% CO_2 for 48 hours after infection and then measured for

467 reporter expression. Reporter expression was determined by measuring the total fluorescent
468 signal intensity of each well using a fluorescence microplate reader at an excitation filter
469 wavelength of 552 nm and an emission filter wavelength of 596 nm.

470 **5.8 Cell viability assays**.

471 Cell viability of TZM-bl cells was determined by monitoring mitochondrial reductase
472 activity from the reduction of the tetrazolium salt MTT by metabolically active cells.[69] TZM-bl
473 cells were plated into 96 well plates (Greiner Bio-One) followed by overnight incubation at
474 37°C, 5% CO_2. Compounds were added to wells with a final DMSO concentration of 1%
475 followed by an additional 48 hours incubation. After the designated incubation time, MTT
476 reagent (5mg/mL in 1x PBS) was added to each well to a final concentration of 0.5 mg/mL.
477 MTT containing plates were incubated for an additional 3 hours after which the media was
478 removed, and the reduced purple formazan product dissolved in 50 µL DMSO. Absorbance was
479 measured at 550 nm. Metabolic activity of vehicle-treated cells (1% DMSO) was defined as
480 100% cell growth. Cell viability of LC5-RIC cultures exposed to HIV inoculum and test
481 compounds was determined by performing a CellTiter-Blue® cell viability assay (Promega) and
482 monitoring the ability of metabolically active cells to convert the redox dye resazurin into the
483 fluorescent product resorufin. LC5-RIC cells were plated into black 96 well plates (Greiner Bio-
484 One) followed by overnight incubation at 37°C, 5% CO_2. Compounds stocks dissolved at 20 mM
485 in DMSO were screened at multiple concentrations from 0.1 to 200 µM at a final DMSO
486 concentration of 1% followed by an additional 48 hours incubation. After the designated
487 incubation time, CTB reagent (1:5 in cell culture medium) was added to each well. CTB
488 containing plates were incubated for an additional hour after which fluorescence signal of

resazurin was measured using a fluorescence microplate reader at an excitation filter wavelength of 550 nm and an emission filter wavelength of 600 nm.

5.9 Time-of-addition assay.

To gain a further understanding of the mechanism of action of the antiviral azaBINOL compound **B#24**, a time-of-addition experiment was employed utilizing single-round HIV-1 pseudo particles.[70, 71] TZM-bl cells were plated into 96 well plates (Greiner Bio-One) followed by overnight incubation at 37°C and 5% CO_2. After 24 hours, plated TZM-bl cell were infected with HIV-1_{YU2} pseudovirus. **B#24** (60 μM), temsavir (40 nM), efavirenz (40 nM), and raltegravir (1 μM) were added to separate wells at the initial viral inoculation time or at set points post-infection (up to 12 hours post-infection). Cells, virus, and inhibitor were incubated for an additional 48 hours followed by quantification of luciferase production to assess viral infection rates. The antiretroviral drug controls chosen (temsavir, efavirenz, raltegravir) reflect inhibition of HIV-1 at different stages of the viral lifecycle (entry/fusion, reverse transcription, and integration, respectively) allowing for a mechanistic comparison to the unknown antiviral compound **B#24**.

5.10 HIV-1 integrase enzyme assay.

Inhibition of HIV-1 integrase was assessed using an HIV-1 integrase assay kit (XpressBio Life Science Products) according to the manufacturer's instructions. IC_{50} values were determined through a two-fold dilution series run in triplicate. The normalized percent integrase inhibition was determined using positive and negative control references with a set amount of vehicle solvent (1% DMSO).

5.11 HIV-1 reverse transcriptase enzyme assay.

Antiviral azaBINOL **B#24** was assessed for inhibition of HIV-1 reverse transcriptase using a commercially available colorimetric reverse transcriptase assay kit (Roche) according to the manufacturer's instructions. IC_{50} values were determined through a dilution series run in triplicate. Normalized percentages of inhibitory activity were calculated using positive and negative control wells with a set amount of vehicle solvent (10% DMSO).

5.12 Polymerase-Independent RNase H assay.

A FRET based assay to assess RNase H inhibition of HIV-1 RT was used as previously described.[40] In a 100 µL reaction containing 50 mM Tris HCl at pH 7.8, 5.8 M $MgCl_2$, 1 M dithiothreitol (DTT), 80 mM KCl, 2 nM HIV-1 RT (NIH Aids Reagent, cat#3555), and 0.25 µM annealed RNA/DNA hybrid (5'-GAU CUG AGC CUG GGA GCU-Fluorescein-3'; 5'-Dabcyl-AGC TCC CAG GCT CAG ATC-3'; Metabion, Germany) was incubated at 37°C for 1 hour. Enzymatic activity was quenched with the addition of 50 µL of ethylenediaminetetraacetic acid (EDTA; 0.5 M, pH 8.0) and fluorescence read using a Biotek plate reader at 490/528 nm excitation/emission wavelength. Data was analyzed by subtracting the value of a vehicle blank (1% DMSO) and reporting inhibitor as a percentage of the control.

5.13 Bio-layer interferometry binding analysis.

Binding of compounds to HIV-1 reverse transcriptase was detected and monitored in real time using a FortéBio Octet Red 96 BioLayer Interferometer. Recombinant wildtype HIV-1 RT (NIH Aids Reagent, cat# 3555) was immobilized on amine reactive sensors (AR2G) at 25 µg/mL for 1600 seconds in 50 mM acetate buffer at a pH of 7. Compounds at 20 mM in DMSO were diluted to final concentrations in black 96 well plates (Greiner Bio-One) at a final consistent DMSO concentration of 5% in 1x kinetic buffer (PBS pH 7.4, 0.02% Tween-20, 0.1% albumin, and 0.05% sodium azide, FortéBio). Binding affinity (K_D) was characterized through the analysis

of association and dissociation curves at multiple concentrations. All samples were tested in duplicate. Rilpivirine was used as a positive binding control, raltegravir as a negative control. Effects from non-specific binding were removed using double referencing. Residual baseline drift was calculated by fitting the response during baseline periods to an exponential decay and then subtracting this drift. The resulting response curves were globally fit to a 1:1 Langmuir model.[72] All fits were performed using a constrained, non-linear least squares minimization (MATLAB R2018a, lsqnonlin function implementing the trust region reflective algorithm). Constraints on parameters were used to guide convergence away from non-physical parameter values, but all constraints were inactive at the converged optimum. A parametric bootstrap analysis was used to compute a 95% confidence interval for the computed K_D values, using a normally-distributed error with variance estimated from the sum of squared residuals of the model fit (MATLAB R2018a, 100 iterations). Random noise in response curves was filtered prior to plotting using a smoothing spline (MATLAB R2018a, spaps function).

5.14 Bivalent metal binding assay.

Testing for complexation of **B#24** with Mg^{2+} ions was carried out following previous protocols with adjustments.[50] In brief, a 1 M stock solution of $MgCl_2$ and a 1 M solution of **B#24** were prepared in 1:1 ethanol/acetonitrile mixtures. **B#24** was diluted to 100 µM and UV absorbance readings recorded using a BioTek synergy plate reader from 200 – 400 nm. 10 µL additions of a 500 mM Mg^{2+} solution containing 100 µM **B#24** (to keep compound concentration consistent) was added stepwise followed by absorbance readings between each addition. The concentration of Mg^{2+} was raised with each addition from 0.5 mM to 120 mM. Alignment, reference subtraction of blanks, and plotting were done on raw data using Microsoft Excel.

5.15 Luminescence inhibition assays.

To determine if **B#24** was capable of non-specifically inhibiting luciferase activity in the HIV-1 pseudotyped assay, we implemented a cell-free assay with purified recombinant luciferase (Promega) and luciferin (BrightGlo Luciferase Assay System; Promega) following a previous protocol.[38] Protein and reagents were prepared and stored according to manufacturer's instructions. Preliminary experiments established the concentration of luciferin to be used in the assay in order to closely mimic the protein signal in single-round infectivity assay and give maximal sensitivity in luminescence readings. Reactions were carried out in white 96 well-plates (Gibco; ThermoFisher Scientific) by combining compounds with 0.5 µg/mL recombinant luciferase in 1x PBS buffer and 1 mg/mL BSA (VWR). Reactions were initiated by the addition of 30 µL luciferin substrate to wells. Luminescence readings were immediately recorded and normalized using appropriate controls with vehicle solvent (1% DMSO). The compounds Luciferase Inhibitor I (VWR) and raltegravir (NIH Aids Reagent Program) were used as positive and negative controls respectively.

5.16 Compound aggregation assessment.

We observed precipitation of some azaBINOL compounds at concentrations higher than 200 µM in cell media with 1% DMSO. To assess if the antiviral activity from the active azaBINOL compound **B#24** could be due to non-specific aggregation effects, an ^{1}H-NMR assay was implemented to characterize compound behavior in aqueous conditions as described previously.[39] Briefly, **B#24** was solubilized in DMSO-D_6 (MilliporeSigma; Burlington, MA) to a concentration of 20 mM. Serial dilution in 50 mM sodium phosphate at pH 6.8 in 100% D_2O (MilliporeSigma; Burlington, MA) yielded five samples ranging in concentration from 200 µM to 12 µM. ^{1}H-NMR spectra of each sample was obtained over 64 scans on a Bruker Ascend 800

579 MHz spectrometer equipped with a 5mm TCI cryoprobe. Data was analyzed and plotted using
580 Bruker TopSpin software.
581
582 **Author contributions**
583 All compounds were synthesized and characterized by SB, SMS, and PRB. All cell-based assays
584 were done by RO, GN, and AH. Data analysis was performed by RO, AH, JS, RBW, PRB and
585 SL. The manuscript was written through contributions of all authors and all authors have given
586 approval to the final version of the manuscript.
587
588 **Acknowledgments**
589 This work was supported by OSU start-up funds (SL). Envelope plasmids (pHxB2, pYU2,
590 p89.6) were a kind gift from Carole Bewley (NIH, NIDDK). Temsavir was kindly provided by
591 Bristol Myers Squibb. This compound has subsequently been by acquired by ViiV Healthcare.
592 The following reagents were obtained through the NIH AIDS Reagent Program, Division of
593 AIDS, NIAID, NIH: TZM-bl cells (Cat# 8129) from Dr. John C. Kappes, Dr. Xiaoyun Wu and
594 Tranzyme Inc. Raltegravir (Cat # 11680) from Merck & Company, Inc. Efavirenz (Cat # 4624)
595 from the Division of AIDS, NIAID. Rilpivirine (Cat # 12147) from Tibotec Pharmaceuticals,
596 Inc. HIV-1 RT (Cat #3555) from Dr. Stuardt Le Grice and Dr. Jennifer T. Miller. We
597 acknowledge the support of the Oregon State University NMR facility funded in part by the
598 National Institutes of Health, HEI Grant 1S110OD018518, and by the M. J. Murdock Charitable
599 Trust grant #2014162.
600
601 **Supplementary data**

602 Supplementary data (additional NMR data and figures illustrating compound library antiviral
603 screening, protein assay results, BLI control data, and assessment of nonspecific inhibition)
604 associated with this article can be found in the online version.
605

606 **References**

607 (1) *HIV/AIDS factsheet*; World Health Organization:
608 http://www.who.int/mediacentre/factsheets/fs360/en/ 2018.

609 (2) Fauci, A. S. An HIV vaccine is essential for ending the HIV/AIDS pandemic. *Jama* **2017,**
610 318, 1535-1536.

611 (3) Pham, Q. D.; Wilson, D. P.; Law, M. G.; Kelleher, A. D.; Zhang, L. Global burden of
612 transmitted HIV drug resistance and HIV-exposure categories: a systematic review and meta-
613 analysis. *AIDS* **2014,** 28, 2751-2762.

614 (4) Tang, M. W.; Shafer, R. W. HIV-1 antiretroviral resistance. *Drugs* **2012,** 72, e1-e25.

615 (5) Miller, C.; Crain, J.; Tran, B.; Patel, N. Rilpivirine: a new addition to the anti-HIV-1
616 armamentarium. *Drugs Today (Barc)* **2011,** 47, 5-15.

617 (6) Murphy, R. L.; Montaner, J. Drug Evaluations Anti-infectives: Nevirapine: A review of its
618 development, pharmacological profile and potential for clinical use. *Expert Opin. Investig.*
619 *Drugs.* **1996,** 5, 1183-1199.

620 (7) De Clercq, E.; Li, G. Approved antiviral drugs over the past 50 years. *Clin. Microbiol. Rev.*
621 **2016,** 29, 695-747.

622 (8) Corona, A.; Masaoka, T.; Tocco, G.; Tramontano, E.; Le Grice, S. F. Active site and
623 allosteric inhibitors of the ribonuclease H activity of HIV reverse transcriptase. *Future Med.*
624 *Chem.* **2013,** 5, 2127-2139.

625 (9) Wang, X.; Gao, P.; Menendez-Arias, L.; Liu, X.; Zhan, P. Update on recent developments
626 in small molecular HIV-1 RNase H inhibitors (2013-2016): opportunities and challenges. *Curr.*
627 *Med. Chem* **2018,** 25, 1682-1702.

628 (10) de Béthune, M.-P. Non-nucleoside reverse transcriptase inhibitors (NNRTIs), their
629 discovery, development, and use in the treatment of HIV-1 infection: a review of the last 20
630 years (1989–2009). *Antivir. Res.* **2010,** 85, 75-90.

631 (11) Beilhartz, G. L.; Götte, M. HIV-1 ribonuclease H: structure, catalytic mechanism and
632 inhibitors. *Viruses* **2010,** 2, 900-926.

633 (12) Brunel, J. M. BINOL: a versatile chiral reagent. *Chem. Rev.* **2005,** 105, 857-897.

634 (13) Aldemir, H.; Richarz, R.; Gulder, T. A. The biocatalytic repertoire of natural biaryl
635 formation. *Angew. Chem. Int. Ed. Engl.* **2014,** 53, 8286-8293.

636 (14) Bringmann, G.; Gulder, T.; Gulder, T. A. M.; Breuning, M. Atroposelective total synthesis
637 of axially chiral biaryl natural products. *Chem. Rev.* **2011,** 111, 563-639.

638 (15) Boyd, M. R.; Hallock, Y. F.; Cardellina, J. H.; Manfredi, K. P.; Blunt, J. W.; McMahon, J.
639 B.; Buckheit Jr, R. W.; Bringmann, G.; Schäffer, M.; Cragg, G. M. Anti-HIV michellamines
640 from Ancistrocladus korupensis. *J. Med. Chem.* **1994,** 37, 1740-1745.

641 (16) Hallock, Y. F.; Manfredi, K. P.; Dai, J.-R.; Cardellina, J. H.; Gulakowski, R. J.; McMahon,
642 J. B.; Schäffer, M.; Stahl, M.; Gulden, K.-P.; Bringmann, G. Michellamines D− F, new HIV-
643 inhibitory dimeric naphthylisoquinoline alkaloids, and korupensamine E, a new antimalarial
644 monomer, from *A*ncistrocladus korupensis. *J. Nat. Prod.* **1997,** 60, 677-683.

645 (17) Manfredi, K. P.; Blunt, J. W.; Cardellina, J. H.; McMahon, J. B.; Pannell, L. L.; Cragg, G.
646 M.; Boyd, M. R. Novel alkaloids from the tropical plant Ancistrocladus abbreviatus inhibit cell
647 killing by HIV-1 and HIV-2. *J. Med. Chem.* **1991,** 34, 3402-3405.

(18) Bringmann, G.; Steinert, C.; Feineis, D.; Mudogo, V.; Betzin, J.; Scheller, C. HIV-inhibitory michellamine-type dimeric naphthylisoquinoline alkaloids from the Central African liana Ancistrocladus congolensis. *Phytochemistry* **2016,** 128, 71-81.

(19) McMahon, J. B.; Currens, M. J.; Gulakowski, R. J.; Buckheit, R.; Lackman-Smith, C.; Hallock, Y. F.; Boyd, M. R. Michellamine B, a novel plant alkaloid, inhibits human immunodeficiency virus-induced cell killing by at least two distinct mechanisms. *Antimicrob. Agents Chemother.* **1995,** 39, 484-488.

(20) Bringmann, G.; Holenz, J.; Wiesen, B.; Nugroho, B. W.; Proksch, P. Diconcophylline A as a growth-retarding agent against the herbivorous insect Spodoptera littoralis: structure-activity relationships. *J. Nat. Prod.* **1997,** 60, 342-437.

(21) Teissier, E.; Zandomeneghi, G.; Loquet, A.; Lavillette, D.; Lavergne, J. P.; Montserret, R.; Cosset, F. L.; Bockmann, A.; Meier, B. H.; Penin, F.; Pecheur, E. I. Mechanism of inhibition of enveloped virus membrane fusion by the antiviral drug arbidol. *PLoS One* **2011,** 6, e15874.

(22) Emileh, A.; Tuzer, F.; Yeh, H.; Umashankara, M.; Moreira, D. R.; Lalonde, J. M.; Bewley, C. A.; Abrams, C. F.; Chaiken, I. M. A model of peptide triazole entry inhibitor binding to HIV-1 gp120 and the mechanism of bridging sheet disruption. *Biochemistry* **2013,** 52, 2245-2261.

(23) Wolf, M. C.; Freiberg, A. N.; Zhang, T.; Akyol-Ataman, Z.; Grock, A.; Hong, P. W.; Li, J.; Watson, N. F.; Fang, A. Q.; Aguilar, H. C.; Porotto, M.; Honko, A. N.; Damoiseaux, R.; Miller, J. P.; Woodson, S. E.; Chantasirivisal, S.; Fontanes, V.; Negrete, O. A.; Krogstad, P.; Dasgupta, A.; Moscona, A.; Hensley, L. E.; Whelan, S. P.; Faull, K. F.; Holbrook, M. R.; Jung, M. E.; Lee, B. A broad-spectrum antiviral targeting entry of enveloped viruses. *Proc. Natl. Acad. Sci. U.S.A.* **2010,** 107, 3157-3162.

(24) Himmel, D. M.; Sarafianos, S. G.; Dharmasena, S.; Hossain, M. M.; McCoy-Simandle, K.; Ilina, T.; Clark Jr, A. D.; Knight, J. L.; Julias, J. G.; Clark, P. K. HIV-1 reverse transcriptase structure with RNase H inhibitor dihydroxy benzoyl naphthyl hydrazone bound at a novel site. *ACS Chem. Biol.* **2006,** 1, 702-712.

(25) Kankanala, J.; Kirby, K. A.; Liu, F.; Miller, L.; Nagy, E.; Wilson, D. J.; Parniak, M. A.; Sarafianos, S. G.; Wang, Z. Design, synthesis, and biological evaluations of hydroxypyridonecarboxylic acids as inhibitors of HIV reverse transcriptase associated RNase H. *J. Med. Chem.* **2016,** 59, 5051-5062.

(26) Banerjee, S.; Riggs, B. E.; Zakharov, L. N.; Blakemore, P. R. Synthesis, properties, and enantiomerization behavior of axially chiral phenolic derivatives of 8-(naphth-1-yl)quinoline and comparison to 7,7'-dihydroxy-8,8'-biquinolyl and 1,1'-bi-2-naphthol. *Synthesis* **2015,** 47, 4008-4016.

(27) Blakemore, P. R.; Kilner, C.; Milicevic, S. D. Harnessing anionic rearrangements on the benzenoid ring of quinoline for the synthesis of 6,6'-disubstituted 7,7'-dihydroxy-8,8'-biquinolyls. *J. Org. Chem.* **2005,** 70, 373-376.

(28) Blakemore, P. R.; Milicevic, S. D.; Zakharov, L. N. Enzymatic resolution of 7,7'-dihydroxy-8,8'-biquinolyl dipentanoate and its conversion to 2,2'-Di-tert-butyl-7,7'-dihydroxy-8,8'-biquinolyl. *J. Org. Chem.* **2007,** 72, 9368-9371.

(29) Wang, C.; Flanigan, D. M.; Zakharov, L. N.; Blakemore, P. R. Synthesis of 7,7'-dihydroxy-8,8'-biquinolyl (azaBINOL) via Pd-catalyzed directed double C-H functionalization of 8,8'-biquinolyl: emergence of an atropos from a tropos State. *Org. Lett.* **2011,** 13, 4024-4027.

(30) Blakemore, P. R.; Kilner, C.; Milicevic, S. D. Resolution, enantiomerization kinetics, and chiroptical properties of 7,7'-dihydroxy-8,8'-biquinolyl. *J. Org. Chem.* **2006,** 71, 8212-8218.

(31) Blakemore, P. R.; Milicevic, S. D.; Perera, H.; Shvarev, A.; Zakharov, L. N. Determination of pKa values for diether derivatives of 7,7'-dihydroxy-8,8'-biquinolyl: dependence of basicity on interannular dihedral angle. *Synthesis* **2008**, 2271-2277.

(32) Sephton, S. M.; Wang, C.; Zakharov, L. N.; Blakemore, P. R. Silylcyanation of aldehydes, ketones, and imines catalyzed by a 6,6'-bis-sulfonamide derivative of 7,7'-dihydroxy-8,8'-biquin-olyl (azaBINOL). *Eur. J. Org. Chem.* **2012,** 2012, 3249-3260.

(33) Wu, Z.; Wang, C.; Zakharov, L. N.; Blakemore, P. R. Enantioselective synthesis of biaryl compounds via Suzuki-Miyaura cross-coupling using a palladium complex of 7'-butoxy-7-(diphenylphosphino)-8,8'-biquinolyl: investigation of a new chiral ligand architecture. *Synthesis* **2014,** 46, 678-685.

(34) Harrigan, P. R.; Stone, C.; Griffin, P.; Nájera, I.; Bloor, S.; Kemp, S.; Tisdale, M.; Larder, B. Resistance profile of the human immunodeficiency virus type 1 reverse transcriptase inhibitor abacavir (1592u89) after monotherapy and combination therapy. *J. Infect. Dis.* **2000,** 181, 912-920.

(35) Kremb, S.; Helfer, M.; Heller, W.; Hoffmann, D.; Wolff, H.; Kleinschmidt, A.; Cepok, S.; Hemmer, B.; Durner, J.; Brack-Werner, R. EASY-HIT: HIV full-replication technology for broad discovery of multiple classes of HIV inhibitors. *Antimicrob. Agents Chemother.* **2010,** 54, 5257-5268.

(36) Baell, J. B. Feeling nature's PAINS: Natural products, natural product drugs, and pan assay interference compounds (PAINS). *J. Nat. Prod.* **2016,** 79, 616-628.

(37) Auld, D. S.; Southall, N. T.; Jadhav, A.; Johnson, R. L.; Diller, D. J.; Simeonov, A.; Austin, C. P.; Inglese, J. Characterization of chemical libraries for luciferase inhibitory activity. *J. Med. Chem.* **2008,** 51, 2372-2386.

(38) Bedford, R.; LePage, D.; Hoffmann, R.; Kennedy, S.; Gutschenritter, T.; Bull, L.; Sujijantarat, N.; DiCesare, J. C.; Sheaff, R. J. Luciferase inhibition by a novel naphthoquinone. *J. Photochem. Photobiol.* **2012,** 107, 55-64.

(39) LaPlante, S. R.; Carson, R.; Gillard, J.; Aubry, N.; Coulombe, R.; Bordeleau, S.; Bonneau, P.; Little, M.; O'Meara, J.; Beaulieu, P. L. Compound aggregation in drug discovery: implementing a practical NMR assay for medicinal chemists. *J. Med. Chem.* **2013,** 56, 5142-5150.

(40) Parniak, M. A.; Min, K.-L.; Budihas, S. R.; Le Grice, S. F.; Beutler, J. A. A fluorescence-based high-throughput screening assay for inhibitors of human immunodeficiency virus-1 reverse transcriptase-associated ribonuclease H activity. *Anal. Biochem.* **2003,** 322, 33-39.

(41) Corona, A.; Tramontano, E. RNase H polymerase-independent cleavage assay for evaluation of RNase H activity of reverse transcriptase enzymes. *Bio Protoc.* **2015,** 5, e1561.

(42) Klumpp, K.; Hang, J. Q.; Rajendran, S.; Yang, Y.; Derosier, A.; Wong Kai In, P.; Overton, H.; Parkes, K. E.; Cammack, N.; Martin, J. A. Two-metal ion mechanism of RNA cleavage by HIV RNase H and mechanism-based design of selective HIV RNase H inhibitors. *Nucleic Acids Res.* **2003,** 31, 6852-6859.

(43) Budihas, S. R.; Gorshkova, I.; Gaidamakov, S.; Wamiru, A.; Bona, M. K.; Parniak, M. A.; Crouch, R. J.; McMahon, J. B.; Beutler, J. A.; Le Grice, S. F. Selective inhibition of HIV-1

reverse transcriptase-associated ribonuclease H activity by hydroxylated tropolones. *Nucleic Acids Res.* **2005,** 33, 1249-1256.

(44) Beilhartz, G. L.; Ngure, M.; Johns, B. A.; DeAnda, F.; Gerondelis, P.; Götte, M. Inhibition of the ribonuclease H activity of HIV-1 reverse transcriptase by GSK5750 correlates with slow enzyme-inhibitor dissociation. *J. Biol. Chem.* **2014,** 289, 16270-16277.

(45) Vernekar, S. K. V.; Tang, J.; Wu, B.; Huber, A. D.; Casey, M. C.; Myshakina, N.; Wilson, D. J.; Kankanala, J.; Kirby, K. A.; Parniak, M. A. Double-winged 3-hydroxypyrimidine-2, 4-diones: potent and selective inhibition against HIV-1 RNase H with significant antiviral activity. *J. Med. Chem.* **2017,** 60, 5045-5056.

(46) Boyer, P. L.; Smith, S. J.; Zhao, X. Z.; Das, K.; Gruber, K.; Arnold, E.; Burke, T. R.; Hughes, S. H. Developing and evaluating inhibitors against the RNase H active site of HIV-1 RT. *J. Virol.* **2018,** 92, 02203-02217.

(47) Tramontano, E.; Esposito, F.; Badas, R.; Di Santo, R.; Costi, R.; La Colla, P. 6-[1-(4-Fluorophenyl) methyl-1H-pyrrol-2-yl)]-2, 4-dioxo-5-hexenoic acid ethyl ester a novel diketo acid derivative which selectively inhibits the HIV-1 viral replication in cell culture and the ribonuclease H activity in vitro. *Antivir. Res.* **2005,** 65, 117-124.

(48) Chung, S.; Wendeler, M.; Rausch, J. W.; Beilhartz, G.; Gotte, M.; O'Keefe, B. R.; Bermingham, A.; Beutler, J. A.; Liu, S.; Zhuang, X. Structure-activity analysis of vinylogous urea inhibitors of human immunodeficiency virus-encoded ribonuclease H. *Antimicrob. Agents Chemother.* **2010,** 54, 3913-3921.

(49) Masaoka, T.; Chung, S.; Caboni, P.; Rausch, J. W.; Wilson, J. A.; Taskent-Sezgin, H.; Beutler, J. A.; Tocco, G.; Le Grice, S. F. Exploiting drug-resistant enzymes as tools to identify thienopyrimidinone inhibitors of human immunodeficiency virus reverse transcriptase-associated ribonuclease H. *J. Med. Chem.* **2013,** 56, 5436-5445.

(50) Poongavanam, V.; Corona, A.; Steinmann, C.; Scipione, L.; Grandi, N.; Pandolfi, F.; Di Santo, R.; Costi, R.; Esposito, F.; Tramontano, E. Structure-guided approach identifies a novel class of HIV-1 ribonuclease H inhibitors: binding mode insights through magnesium complexation and site-directed mutagenesis studies. *MedChemComm* **2018,** 9, 562-575.

(51) Wendeler, M.; Lee, H.-F.; Bermingham, A.; Miller, J. T.; Chertov, O.; Bona, M. K.; Baichoo, N. S.; Ehteshami, M.; Beutler, J.; O'keefe, B. R. Vinylogous ureas as a novel class of inhibitors of reverse transcriptase-associated ribonuclease H activity. *ACS Chem. Biol.* **2008,** 3, 635-644.

(52) Corona, A.; Desantis, J.; Massari, S.; Distinto, S.; Masaoka, T.; Sabatini, S.; Esposito, F.; Manfroni, G.; Maccioni, E.; Cecchetti, V. Studies on cycloheptathiophene-3-carboxamide derivatives as allosteric HIV-1 ribonuclease H inhibitors. *ChemMedChem* **2016,** 11, 1709-1720.

(53) Massari, S.; Corona, A.; Distinto, S.; Desantis, J.; Caredda, A.; Sabatini, S.; Manfroni, G.; Felicetti, T.; Cecchetti, V.; Pannecouque, C. From cycloheptathiophene-3-carboxamide to oxazinone-based derivatives as allosteric HIV-1 ribonuclease H inhibitors. *J. Enzyme Inhib. Med. Chem.* **2019,** 34, 55-74.

(54) Shah, N. B.; Duncan, T. M. Bio-layer interferometry for measuring kinetics of protein-protein interactions and allosteric ligand effects. *J. Vis. Exp.* **2014**, e51383.

(55) Kwong, P. D.; Wyatt, R.; Robinson, J.; Sweet, R. W.; Sodroski, J.; Hendrickson, W. A. Structure of an HIV gp120 envelope glycoprotein in complex with the CD4 receptor and a neutralizing human antibody. *Nature* **1998,** 393, 648-659.

(56) Richman, D. D.; Wrin, T.; Little, S. J.; Petropoulos, C. J. Rapid evolution of the neutralizing antibody response to HIV type 1 infection. *Proc. Natl. Acad. Sci. U.S.A.* **2003,** 100, 4144-4149.

(57) Kwong, P. D.; Mascola, J. R.; Nabel, G. J. Broadly neutralizing antibodies and the search for an HIV-1 vaccine: the end of the beginning. *Nat. Rev. Immunol.* **2013,** 13, 693-701.

(58) Sluis-Cremer, N.; Arion, D.; Parniak, M. A. Destabilization of the HIV-1 reverse transcriptase dimer upon interaction with N-acyl hydrazone inhibitors. *Mol. Pharmacol.* **2002,** 62, 398-405.

(59) Vernekar, S. K. V.; Liu, Z.; Nagy, E.; Miller, L.; Kirby, K. A.; Wilson, D. J.; Kankanala, J.; Sarafianos, S. G.; Parniak, M. A.; Wang, Z. Design, synthesis, biochemical, and antiviral evaluations of C6 benzyl and C6 biarylmethyl substituted 2-hydroxylisoquinoline-1, 3-diones: dual inhibition against HIV reverse transcriptase-associated RNase H and polymerase with antiviral activities. *J. Med. Chem.* **2014,** 58, 651-664.

(60) Hang, J. Q.; Li, Y.; Yang, Y.; Cammack, N.; Mirzadegan, T.; Klumpp, K. Substrate-dependent inhibition or stimulation of HIV RNase H activity by non-nucleoside reverse transcriptase inhibitors (NNRTIs). *Biochem. Biophys. Res. Commun.* **2007,** 352, 341-350.

(61) Bringmann, G.; Gunther, C.; Ochse, M.; Schupp, O.; Tasler, S. Biaryls in nature: a multi-facetted class of stereochemically, biosynthetically, and pharmacologically intriguing secondary metabolites. *Prog. Chem. Org. Nat. Prod.* **2001,** 82, 1-293.

(62) Platt, E. J.; Bilska, M.; Kozak, S. L.; Kabat, D.; Montefiori, D. C. Evidence that ecotropic murine leukemia virus contamination in TZM-bl cells does not affect the outcome of neutralizing antibody assays with human immunodeficiency virus type 1. *J. Virol.* **2009,** 83, 8289-8292.

(63) Platt, E. J.; Wehrly, K.; Kuhmann, S. E.; Chesebro, B.; Kabat, D. Effects of CCR5 and CD4 cell surface concentrations on infections by macrophagetropic isolates of human immunodeficiency virus type 1. *J. Virol.* **1998,** 72, 2855-2864.

(64) Takeuchi, Y.; McClure, M. O.; Pizzato, M. Identification of gammaretroviruses constitutively released from cell lines used for human immunodeficiency virus research. *J. Virol.* **2008,** 82, 12585-12588.

(65) Wei, X.; Decker, J. M.; Liu, H.; Zhang, Z.; Arani, R. B.; Kilby, J. M.; Saag, M. S.; Wu, X.; Shaw, G. M.; Kappes, J. C. Emergence of resistant human immunodeficiency virus type 1 in patients receiving fusion inhibitor (T-20) monotherapy. *Antimicrob. Agents Chemother.* **2002,** 46, 1896-1905.

(66) Derdeyn, C. A.; Decker, J. M.; Sfakianos, J. N.; Wu, X.; O'Brien, W. A.; Ratner, L.; Kappes, J. C.; Shaw, G. M.; Hunter, E. Sensitivity of human immunodeficiency virus type 1 to the fusion inhibitor T-20 is modulated by coreceptor specificity defined by the V3 loop of gp120. *J. Virol.* **2000,** 74, 8358-8367.

(67) Le Grice, S. F.; Cameron, C. E.; Benkovic, S. J. Purification and characterization of human immunodeficiency virus type 1 reverse transcriptase. In *Methods in enzymology*, Elsevier: 1995; Vol. 262, pp 130-144.

(68) Montefiori, D. C. Evaluating neutralizing antibodies against HIV, SIV, and SHIV in luciferase reporter gene assays. *Curr. Protoc. Immnol.* **2005**, 12.11.11-12.11.17.

(69) Mosmann, T. Rapid colorimetric assay for cellular growth and survival: application to proliferation and cytotoxicity assays. *J. Immunol. Methods* **1983,** 65, 55-63.

(70) Baldick, C. J.; Wichroski, M. J.; Pendri, A.; Walsh, A. W.; Fang, J.; Mazzucco, C. E.; Pokornowski, K. A.; Rose, R. E.; Eggers, B. J.; Hsu, M.; Zhai, W.; Zhai, G.; Gerritz, S. W.; Poss, M. A.; Meanwell, N. A.; Cockett, M. I.; Tenney, D. J. A novel small molecule inhibitor of hepatitis C virus entry. *PLoS Pathog* **2010,** 6, e1001086.

(71) Lara, H. H.; Ayala-Nuñez, N. V.; Ixtepan-Turrent, L.; Rodriguez-Padilla, C. Mode of antiviral action of silver nanoparticles against HIV-1. *J. Nanobiotechnology.* **2010,** 8, 1-10.

(72) Oshannessy, D. J.; Brighamburke, M.; Soneson, K. K.; Hensley, P.; Brooks, I. Determination of rate and equilibrium binding constants for macromolecular interactions using surface plasmon resonance: use of nonlinear least squares analysis methods. *Anal. Biochem.* **1993,** 212, 457-468.

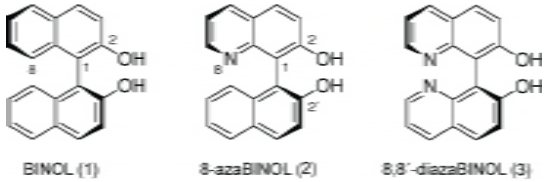

Figure 1. 1,1´-Bi-2-naphthol (BINOL, **1**) and related 8-(naphth-1-yl)quinoline (**2**) and 8,8'-biquinolyl (**3**) compounds belonging to the 'azaBINOL' class. The colloquial names '8-azaBINOL' and '8,8´-diazaBINOL' conform to BINOL atom numbering. Molecules are depicted in (*aS*)-configuration and can exist in racemic or scalemic form.

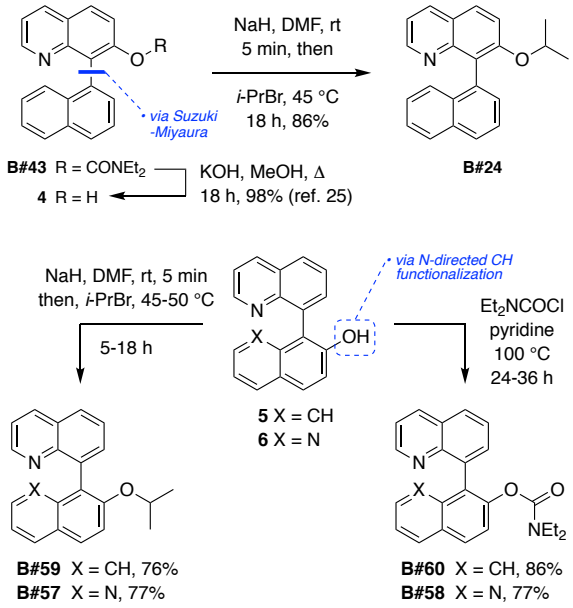

Scheme 1. Synthesis of deoxy-8-azaBINOL (**B#24**, **B#43**, **B#59**, and **B#60**) and 2-deoxy-8,8´-diazaBINOL (**B#57** and **B#58**) derivatives of primary interest for antiviral activity evaluation.

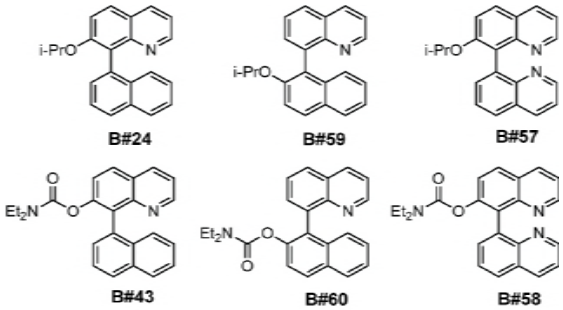

Figure 2. Structures of selected azaBINOL compounds from synthetic library that show significant antiviral activity at single dose concentrations (**B#24**, **B#43**, **B#60**) along with closely related congeners showing only modest antiviral activity (**B#59**, **B#58**, **B#57**).

Compound	HIV-IC_{50} [μM] HxB2	YU2	89.6	CC_{50} [μM] TZM-bl	Selectivity Index CC_{50}/IC_{50}
B#24	6.7 ± 0.9	8.9 ± 0.6	4.7 ± 1.6	68.5 ± 17.1	14.6
B#59	>100	>100	>100	>100	---
B#57	No effect	No effect	No effect	No effect	---
B#43	61.4 ± 3.3	77.6 ± 10.8	56.6 ± 0.8	95.0 ± 13.1	1.7
B#60	12.6 ± 1.6	14.0 ± 0.8	16.8 ± 3.0	69.3 ± 4.9	5.5
B#58	No effect	No effect	No effect	No effect	---

Table 1. HIV-1 pseudo-viral assay determined IC_{50} and CC_{50} for selected azaBINOLs.

Compound	IC_{50} [μM] HIV-1_{IIIB}	CC_{50} [μM] LC5-RIC	Selectivity Index CC_{50}/IC_{50}
B#24	7.6 ± 0.2	86.5 ± 3.7	11.4
B#59	39.5 ± 1.7	144 ± 7.7	3.6
B#57	No effect	No effect	---
B#43	24.1 ± 0.7	51.9 ± 1.2	2.2
B#60	50.1 ± 3.7	71.4 ± 2.8	1.4
B#58	No effect	382.8 ± 166.2	---

Table 2. EASY-HIT HIV-1 assay determined IC_{50} and CC_{50} for selected azaBINOLs.

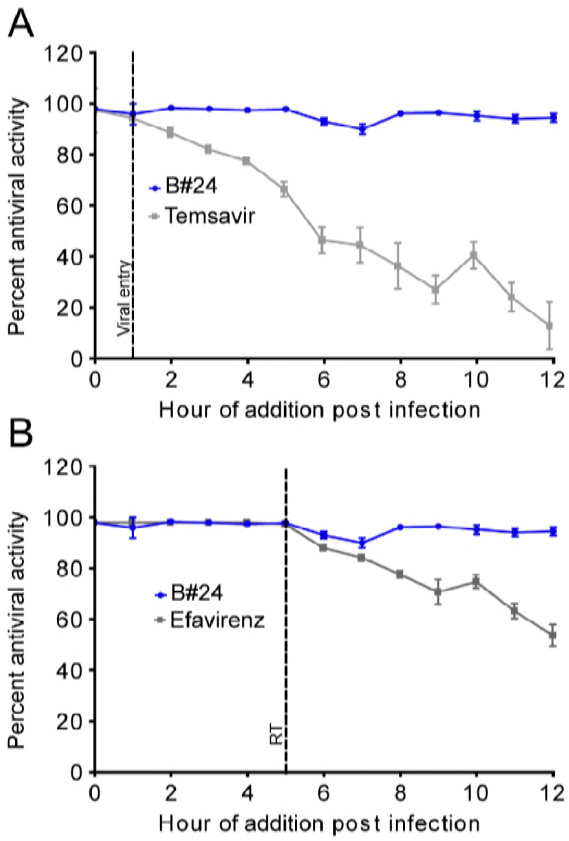

Figure 3. Time-of-addition analysis comparing HIV-1 antiviral activity of **B#24** to antiviral controls at various time points post-infection. TZM-bl cells were infected with HIV-1_{YU2} followed by inoculation with antiviral agents at the indicated time points. A) **B#24** activity profile was compared to an attachment inhibitor (temsavir, 40 nM) and B) a NNRTI (efavirenz, 40 nM). Results are presented as the mean ± S.D. (*error bars*) of triplicates (n = 3).

	HIV-1 Integrase	HIV-1 RT	HIV-1 RNase H	*E. coli* RNase H	MuLV RNase H	AMV RNase H
B#24	>100 µM	>100 µM	14.2 ± 2.8 µM	44.3 ± 6.4 µM	>100 µM	>100 µM
B#57	>100 µM	>100 µM	>100 µM	>100 µM	>100 µM	>100 µM
Rilpivirine	-	~1 nM	>10 µM	>10 µM	>10 µM	>10 µM
Raltegravir	1.1 ± 0.2 µM	-	-	-	-	-

Table 3. **B#24** shows specific inhibition against RNase H with an IC_{50} of 14.2 ± 2.8 µM. **B#57** does not show inhibition against any enzyme tested. Data shown represent mean ± S.D. (*error bars*) of triplicates (n = 3).

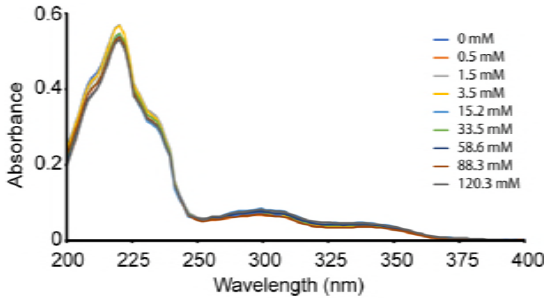

Figure 4. Mg^{2+} ion chelation assay. UV absorbance spectra of **B#24** (100 µM) in the presence of varying concentrations of Mg^{2+} ion. No concentration dependent change of absorbance of **B#24** was seen at any wavelength scanned.

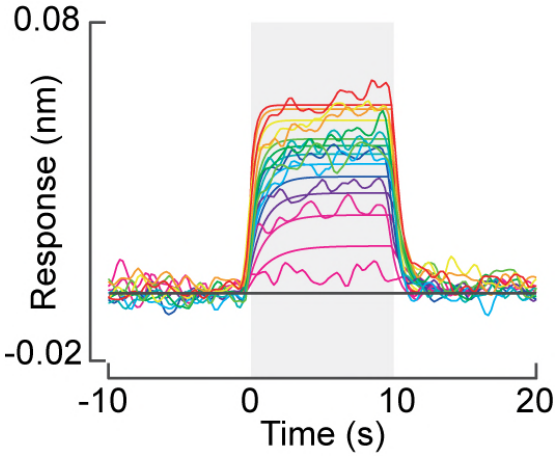

Figure 5. BLI response of inhibitor **B#24** binding to HIV-1 RT enzyme. **B#24** shows a dose-dependent binding to HIV-1 RT with a K_D of 38 µM with a 95% confidence interval between 36 – 41 µM. **B#24** was analyzed at 11 concentrations: 10, 20, 30, 40, 50, 60, 70, 80, 120, 160, and 200 µM. Data was fit globally using a 1:1 binding model.